Improvement of Creep Strength of a Third Generation, Single-Crystal Ni-Base Superalloy by Solution Heat Treatment

G.E. Fuchs

(Submitted 21 February; in revised form 25 July 2001)

The standard solution heat treatment of the third generation, single-crystal Ni-base superalloy, CMSX-10, requires multiple steps at temperatures up to 1365 °C and lasts a total of approximately 45 hours. These high temperatures and long hours result in a heat treatment that is costly. Reducing the temperature and/or time of the heat treatment to reduce the cost of the heat treatment would result in residual segregation of W and Re to the dendrite cores, a locally unstable microstructure. Therefore, a modified heat treatment was evaluated that increased the maximum heat-treatment temperature and the amount of time at the higher heat-treatment temperatures. The microstructures and mechanical properties were evaluated for samples given both the standard and the modified solution heat treatment.

Keywords: creep properties, heat treatment, superalloys

1. Introduction

The development of directional solidification to produce single-crystal turbine blades and vanes has resulted in dramatic improvements in the performance of gas turbines.[1] Single-crystal alloys, which have reduced levels of the grain-boundary elements, such as B, Zr, and Hf, tend to exhibit increased solidus temperatures. The increased melting temperature of single-crystal alloys frequently allows for increased levels of microstructural refinement of the γ' with a solution-anneal heat treatment followed by one or more aging heat treatments. In alloys with a high volume fraction of γ/γ' eutectic after casting, the complete dissolution of γ' by the appropriate heat treatment is of extreme importance for improved mechanical properties.[2]

The solution heat treatment, in addition to dissolving the eutectic γ/γ' and solutioning the γ' for subsequent reprecipitation, also reduces the chemical segregation of the elements.[3] Some elements, during solidification, partition to the dendrite core. Other elements tend to accumulate in the interdendritic liquid and then solidify in the interdendritic and eutectic regions. Tungsten (W) and rhenium (Re), for example, are reported to partition to the dendrite core, whereas tantalum (Ta), aluminum (Al), and titanium (Ti) partition to the interdendritic region.[4,5] In general, the refractory metal-alloy additions have continued to increase as new superalloys have been developed. In particular, the levels of W, Re, and Ta have increased steadily in the first three generations of single-crystal Ni-base superalloys.[6] These increased refractory elements result in alloys with increased strength and creep resistance due to increased solid solution strengthening, strengthening of the γ', and slowed diffusion rates.

The increased refractory-metal contents of the second- and third-generation, single-crystal superalloys, which result in slowed diffusion rates, also resulted in slowed diffusion during solution heat treatments and, therefore, increased heat-treatment temperatures and times. Several attempts have been made to reduce the cost of solution heat treatments of single-crystal alloys by reducing both the heat-treatment temperatures and hold times at elevated temperature.[7] However, previous studies have indicated that shortening the heat-treatment times and/or reducing the heat-treatment temperatures for CMSX-10 would not result in complete homogenization.[8] Although complete γ' solutioning, including the γ/γ' eutectic, occurred at a relatively low temperature (i.e., 1352 °C), a significant amount of segregation remained to much higher heat-treatment temperatures. The segregation of W and Re to the dendrite cores was not reduced until temperatures in excess of 1360 °C. Some residual W and Re segregation was still observed after the heat treatment was complete. Previous studies have shown that increased homogenization heat-treatment temperatures resulted in increased homogeneity and improved creep resistance in early generation single-crystal superalloys with relatively low refractory-metal contents.[9] Therefore, a modified solution heat treatment was evaluated for CMSX-10. Instead of shortening the heat-treatment cycle or using a lower temperature, the heat-treatment time was maintained as constant and the heat-treatment temperatures were modified to result in improved homogenization. The maximum heat-treatment temperature was increased from 1365 to 1370 °C, and the amount of time samples were heat treated at temperatures above 1360 °C was increased from 25 to 30 h. The effect of this modified heat treatment on the tensile and creep properties was determined and compared to samples given the conventional heat treatment.

G.E. Fuchs, Materials Science and Engineering Department, University of Florida, P.O. Box 116400, Rhines Hall, Gainesville, FL, 32611-6400. Contact e-mail: gefuchs@ufl.edu.

2. Materials and Experimental Procedures

The composition of the third-generation, single-crystal Ni-base superalloy, CMSX-10, master heat used in this investigation is shown in Table 1. Single crystals of the alloys were produced in an investment casting cluster mold with 19 bars (1.27 mm in diameter and 200 mm long) at PCC Airfoils (Minerva, OH). The single-crystal samples were cast in the <001> direction in a temperature gradient of 5 to 10 °C/cm and at a constant withdrawal rate of 20 cm/h. The orientation of each bar was determined by Laue back-reflection techniques. Only samples with orientations within 5 deg of <001> and without defects, such as slivers, freckles, low angle boundaries, or high angle boundaries, were used in this investigation. Approximately 2.5 cm long samples were sectioned from the bars by a diamond cutoff wheel and used for metallographic studies. Metallography samples were examined in the as-cast condition after receiving the standard and modified heat treatments. The sample identifications were based on the solution heat treatment. Therefore, the samples designated "Alt" were given the alternate heat treatment, whereas all other samples were given the standard heat treatment (Table 2). Note that the modified solution anneal includes increased maximum heat-treatment temperatures. In addition, the amount of time that the samples were heat treated at or above 1360 °C increased from 25 h in the standard solution anneal to 30 h in the modified heat treatment. All heat treatments were performed in a laboratory vacuum furnace operating at a maximum pressure of 1×10^{-2} Pa. All samples were cooled from the last heat-treatment step by argon quench (gas furnace quench), which produced an initial cooling rate of 250 °C/min. These rapid cooling rates were used to prevent the growth of the γ' during cooling. The temperatures were measured by two Pt/Pt-10Rh thermocouples and were maintained within ±3 °C throughout the heat treatments.

All samples were given the same three-step aging heat treatment to produce a coarse γ' with 0.5 μm edge dimension and fine γ' in the γ channels. All samples were heat treated in air and air-cooled (AC) from the heat-treatment temperature. The temperatures were measured by two Chromel/Alumel thermocouples and were maintained within ±10 °C throughout the heat treatments. The aging heat treatments used in this study were 1150 °C/4 h/AC + 870 °C/24 h/AC + 760 °C/30 h/AC.

The microstructure of the as-cast and heat-treated samples was examined after etching with Pratt and Whitney Etch #17 (100 mL H_2O + 100 mL HCl + 100 mL HNO_3 + 3 g MoO_3), which dissolves the γ'. The microstructures were characterized by light optical microscopy (LOM) and scanning electron microscopy (SEM) metallographic techniques.

The effect of the alternate solution heat treatment on the homogenization was determined and compared to the standard heat treatment. The composition of various phases and microstructural features was determined by microprobe techniques on polished, but unetched microstructural samples. All samples were examined in the solution heat-treated condition. A 1 μm spot size was used for all microprobe characterization to simultaneously sample both the γ and γ' phases and obtain a more representative average composition. Note that the average γ' size following the argon quench was approximately 0.3 μm. Line scans were performed on samples given the standard and alternate solution heat treatments. The line scans utilized a 1 μm spot size, with a 25 μm spacing between measurements along a 1000 μm long line. A minimum of five line scans was performed on each sample, and the average values and the variations are reported. Although the average compositional values are of interest, the variations in composition provided more useful information. The variation in composition, from minimum to maximum, provided an estimate of the elemental segregation. For example, the Ta content would be expected to be a maximum in the interdendritic region but a minimum in the dendrite core. Diffusion that occurs during the solution heat treatment would be expected to reduce the compositional variations and result in a more homogeneous chemical distribution of the elements. Therefore, the differences between the maximum and minimum compositional values, or compositional variations, were used to establish both the initial as-cast and residual segregation following heat treatment.

Differential thermal analysis (DTA) was performed in a DuPont (Philadelphia, PA) 9000 series differential thermal analyzer on samples given either the standard or alternate solution heat treatment to determine the solidus, liquidus, γ' solvus, and eutectic melting point. Prior to the testing of the samples, the DTA unit was calibrated with high-purity Ni at a scan rate of 20 °C/min. All tests were performed in a purged high-purity argon atmosphere with a flow rate of approximately 50 cm^3/min. High-purity alumina crucibles were used

Table 1 Composition (in Weight Percent) of CMSX-10 (Heat VG-254) Used in This Study

Ni	Cr	Co	Mo	W	Ta	Re	Nb	Al	Ti	Hf	C	B	Zr
Bal.	3.30	2.20	0.41	5.60	8.40	6.40	0.10	5.74	0.23	0.04	0.001	0.002	0.001

Table 2 Solution Heat-Treatment Schedule for CMSX-10 Samples Used in This Study

Sample ID	Heat Treatment (a)
Standard	1315 °C/1 h → 1329 °C/2 h → 1335 °C/2 h → 1340 °C/2 h → 1346 °C/2 h → 1352 °C/3 h → 1357 °C/3 h → 1360 °C/5 h → 1363 °C/10 h → 1365 °C/15 h/GFC
Alternate	1315 °C/1 h → 1330 °C/2 h → 1335 °C/2 h → 1340 °C/2 h → 1345 °C/2 h → 1350 °C/2 h → 1355 °C/3 h → 1360 °C/10 h → 1365 °C/10 h → 1370 °C/10 h/GFC

(a) GFC, gas furnace quench.

for all samples. Because of the severe segregation that occurs in these alloys,[10] cylindrical samples with a minimum size of 250 mg (approximately 4 mm diameter × 4 mm length) were used. Data were acquired only on heating to better characterize the effect of the thermal processing and to avoid the effects of supercooling. All samples were heated at a constant 20 °C/min rate, and duplicate samples were evaluated for each condition.

After aging, tensile and creep samples were prepared from material given the standard and the alternate solution heat treatment. Threaded mechanical test samples were low stress ground to final dimensions, with a 4.5 mm diameter × 12.7 mm long gauge section. Tensile samples were tested in the temperature range 25 to 1100 °C in air at an initial strain rate of 1.67×10^{-3}/s. Three samples were tested at each condition, and the results reported are the average of the three tests. The creep samples were tested in constant load conditions at 850, 950, and 1100 °C in air at stresses ranging from 100 to 600 MPa. Similar to the tensile testing, the average of three samples tested under similar conditions was determined for each test temperature and stress. The fracture surfaces were examined by SEM, and some samples were evaluated by transmission electron microscopy (TEM) techniques. The microstructures of the creep samples in both the gauge section and the grip region were evaluated to examine the thermal stability of the samples.

Metallography samples were also given long-term heat treatments at 950 and 1050 °C in order to determine the thermal stability of the alloys, as a function of solution heat treatment. Samples were heat treated for 1000 and 10,000 h at each temperature. The samples were metallographically prepared, as described previously, and examined using SEM techniques. The microstructures of the long-term heat-treated samples were compared to the creep samples.

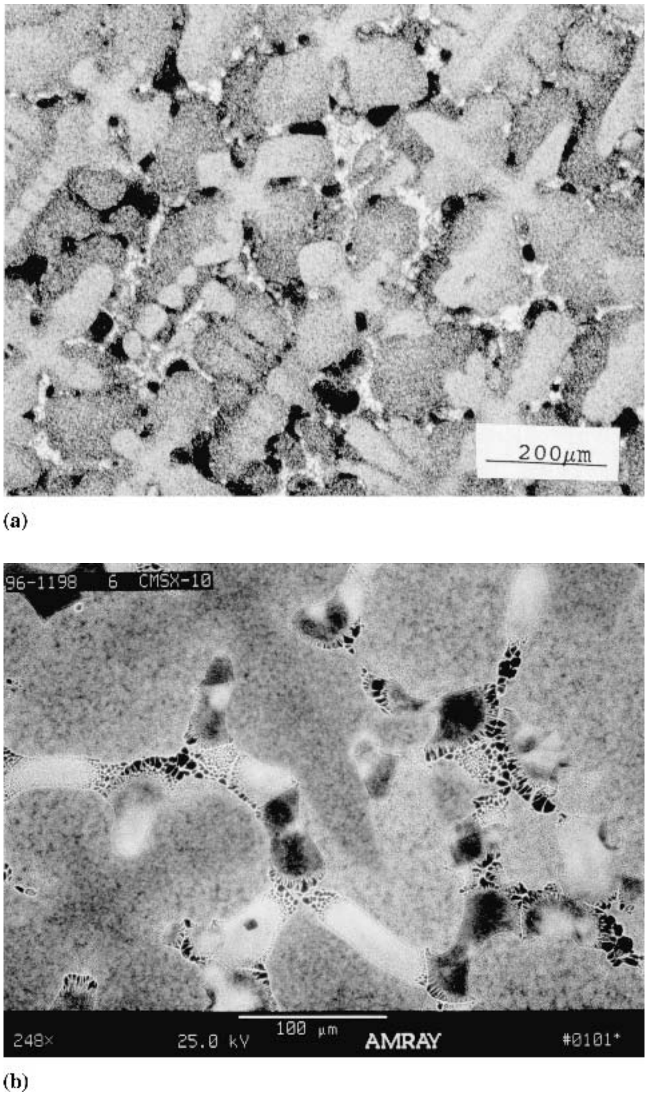

Fig. 1 Photomicrographs of as-cast CMSX-10. (a) In the optical photomicrograph, the dendrites appear medium gray, the interdendritic regions are light gray, and the eutectic areas are black. (b) In the SEM photomicrograph, the eutectic regions are light gray, and the interdendritic areas are relatively coarse.

3. Results

3.1 Microstructure

The as-cast CMSX-10 sample exhibited a two-phase γ/γ' microstructure with a dendritic segregation pattern and a limited amount of γ/γ' eutectic solidification occurring in some interdendritic areas (Fig. 1). The average volume fraction of the γ/γ' eutectic in the as-cast microstructure was approximately 12%. The composition of the dendritic and interdendritic regions was determined by electron microprobe. In comparison to the bulk alloy composition, the dendrite cores were significantly enriched in W and Re and depleted in Ta, Al, and Ti (Table 3). Conversely, the interdendritic region of the as-cast microstructure was enriched in Al, Ti, and Ta, whereas lower levels of W and Re were observed. The eutectic γ/γ' regions were further enriched in Ta, Al, and Ti and depleted in W and Re. Elements, such as Co, Cr, and Mo, did not exhibit any significant degree of segregation to either the dendrite core or the interdendritic regions during solidification. These results are similar to those reported for the model third-generation, single-crystal alloy, SX-1.[11] Microprobe analysis (Table 3) of the solution heat-treated samples was performed to determine the degree of segregation that persisted after either solution heat treatment. For simplicity, only the compositional levels and the variations of the most strongly partitioning elements are reported (i.e., Re, W, Al, Ta, and balance Ni). After the standard solution heat treatment, all of the elements appeared to exhibit much more uniform distributions with only limited variations. However, the W and Re still appeared to exhibit the greatest degree of segregation. A further reduction in the variation of all of the elements was observed following the alternate solution heat treatment.

Table 3 Effect of Solution Heat Treatment on the Liquidus, Solidus, and γ'-Solvus Temperatures (°C) for CMSX-10 (VG-254) as Determined by DTA

Solution Heat Treatment	Liquidus	Solidus	γ'-Solvus
Standard [8]	1419	1390	1344
Alternate	1420	1392	1345

The solution heat treatments dissolved the γ' formed during cooling from solidification and the eutectic γ/γ', and reduced the degree of chemical segregation due to the partitioning of some of the elements to the dendrite core and interdendritic regions. Examination of the microstructures of the heat-treated samples indicated that the γ' was completely solutioned by both heat treatments. After the complete standard heat treatment, at a maximum temperature of 1365 °C, no obvious chemical segregation could be observed in optical and SEM metallographic samples (Fig. 2). The higher temperatures of the alternate solution heat treatment did not have any obvious effects on the samples examined by optical and SEM techniques (Fig. 3).

The DTA testing of the as-cast samples indicated that the liquidus was 1414 °C and the solidus was 1366 °C. Note that the measured solidus is approximately equal to the maximum heat treatment in the standard solution heat treatment (Table 4). No evidence of the γ' solvus was observed in the DTA data from the as-cast material.

The DTA testing indicated that significant changes in the phase-transformation temperatures of the CMSX-10 samples were observed after both solution heat treatments (Table 4). The liquidus and solidus temperatures both increased after heat treatment. The maximum in the solidus temperature (i.e., 1390 °C) was observed at the final standard heat-treatment step at 1365 °C. A slightly higher solidus (i.e., 1392 °C) was observed in the samples given the alternate solution heat treatment. The γ'-solvus temperature was also affected by heat treatment, but was similar in both the standard and alternate solution heat-treatment samples. Although the γ' solvus was not observed in the as-cast samples, the γ'-solvus temperature was detected in all of the heat-treated material. The γ'-solvus temperature was observed at about 1345 °C following either solution heat treatment. The liquidus of the solution heat-treated samples was greater than that of the as-cast material. However, the liquidus of the standard solution heat-treated material was similar to that of material given the alternate solution heat treatment.

3.2 Tensile Properties

The tensile properties (Table 5) of the samples given the alternate solution heat treatment were slightly greater than those of the standard solution heat-treated samples at temperatures up to 850 °C. As is typically observed in Ni-base superalloys, the yield and ultimate tensile strengths increased with increasing temperature, up to a peak of about 850 °C. The increase in the yield stress is attributed to the anomalous increase in flow stress of the γ' precipitate with increasing temperature. The increased ultimate tensile strength also results from an increased amount of work hardening that can occur with increased ductility. The ultimate tensile strength, typically, was observed at failure. No necking was observed prior to fracture. At test temperatures above 850 °C, much less work hardening was observed, but necking still did not occur.

At room temperature and 600 °C, the yield strengths, ulti-

Table 4 Compositional Variations in As-Cast and Heat-Treated Samples of CMSX-10 (VG-254) (a)

Solution Heat Treatment	Ni	Re	W	Al	Ta
As-cast	67.66 ± 1.39	9.28 ± 1.86	7.25 ± 1.18	7.34 ± 1.39	8.52 ± 1.48
Standard	72.17 ± 0.43	6.25 ± 0.25	6.11 ± 0.14	6.61 ± 0.21	8.38 ± 0.16
Alternate	70.98 ± 0.32	6.51 ± 0.19	6.00 ± 0.12	6.48 ± 0.13	8.81 ± 0.10

(a) For clarity, only the most strongly partitioning elements are reported.

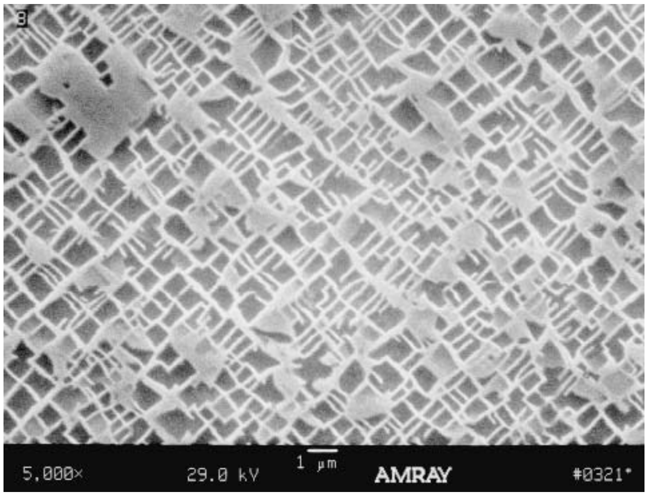

Fig. 2 The SEM photomicrograph of the homogeneous γ' distribution after complete standard solution anneal heat treatment

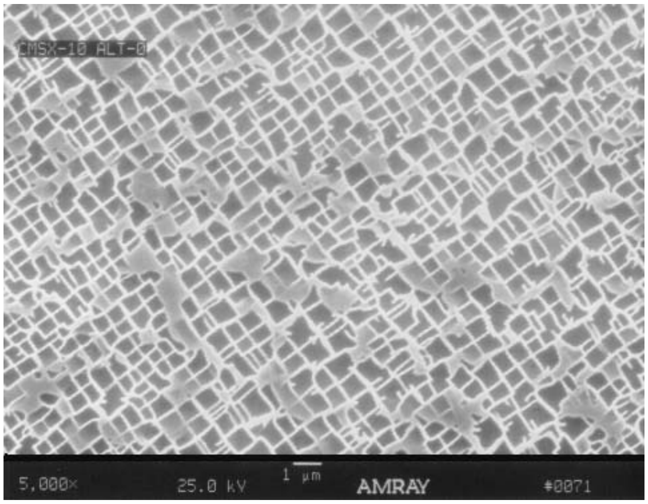

Fig. 3 The SEM photomicrograph of the homogeneous γ' distribution after complete modified solution anneal heat treatment

mate tensile strengths, and ductilities were similar for samples given either solution anneal. However, at 850 °C, the yield strength and ductility of the sample given the alternate solution anneal were greater than those of the conventionally heat-treated sample (1033 versus 875 MPa). The ultimate tensile strength of both samples was similar at 850 °C. At 950 °C, the strength of both samples was very similar. However, the ductility of the modified solution heat-treated sample was greater than that of the standard heat-treated sample (36.7% versus 28.4%). At higher test temperatures, the standard solution heat-treated samples exhibited strengths somewhat greater than the alternate solution heat-treated materials. The ductility of the alternate solution heat-treated samples was superior to that of the standard solution heat-treated samples at all test temperatures. As noted previously, three samples were tested at each condition. Only a limited amount of scatter was observed in the strengths and ductilities determined for both conditions. The solution heat treatment did not appear to have any effect on the degree of scatter in the results.

3.3 Creep Properties

The samples given the alternate solution heat treatment exhibited much greater creep strengths and ductilities than the standard solution heat-treated samples at all test temperatures and stress levels (Table 6 and Fig. 4). At 850 °C, samples given the standard solution heat treatment exhibited creep lives of 237.7 to 294.4 h when tested at a stress of 586 MPa, whereas rupture occurred in similar stressed samples given the alternate solution anneal in 371.9 to 423.8 h. Similarly, at all of the stress levels tested at 950 °C, the samples given the alternate solution heat treatments exhibited longer creep lives than the standard samples. Samples tested at 1100 °C also exhibited a similar trend, but the improvement in creep strength of the modified solution-annealed samples appeared to be less than at lower test temperatures. At creep stresses of 103 MPa, the standard heat-treated samples exhibited creep lives of 651.8 to 722.6 h. However, the samples given the alternate solution anneal exhibited creep lives of about 728.6 h. In general, the higher solution heat-treatment temperature appeared to result in an increase in creep-rupture life under the conditions tested. However, the amount of the increase in creep resistance observed in the samples given the alternate solution heat treatment appeared to decrease with increasing test temperature. The creep ductility of the alternate solution heat treatment was also superior to that of the standard solution heat-treated samples (Table 6 and Fig. 4) under all test conditions examined. The creep properties are plotted on a Larson-Miller, time-temperature-parameter plot in Fig. 4. Note that there was insufficient data to determine the *C* constant for the Larson-Miller plot, so a value of 20 was assumed for *C*. Some scatter in the creep lives and the time to a given amount of creep strain was observed within the groups

Table 5 Tensile Properties of CMSX-10 Samples Given Standard and Alternate Solution Heat Treatments

Test Temperature (°C)	Standard Solution Heat Treatment			Alternate Solution Heat Treatment		
	YS (MPa)	UTS (MPa)	Elongation	YS (MPa)	UTS (MPa)	Elongation
25	812	891	28.8%	807	883	25.4%
600	868	991	16.0%	874	1020	14.7%
850	875	1013	22.8%	1033	1090	27.1%
950	721	815	28.4%	703	833	36.7%
100	453	495	24.9%	413	514	34.8%

Table 6 Creep Properties of CMSX-10 Samples Given Standard and Alternate Solution Heat Treatments

Solution Heat Treatment	Test Temperature (°C)	Creep Stress (MPa)	Time to				Elongation
			Creep Strain			Rupture	
			0.1%	0.2%	1.0%		
Standard	850	586	1.0	1.4	3.4	294.2	31.3%
		586	0.9	1.3	7.0	237.7	29.4%
	950	414	1.3	3.8	15.0	77.4	26.9%
		379	4.1	12.7	46.2	177.2	24.4%
		310	21.2	55.8	136.3	415.2	30.8%
		310	15.9	46.1	167.3	500.5	34.2%
		241	34.2	205.2	552.3	1087.4	29.8%
		241	46.8	266.7	540.9	1079.3	27.9%
	1100	103	5.3	31.9	389.8	722.6	25.8%
		103	17.1	48.2	329.9	651.8	30.3%
Alternate	850	586	1.2	1.6	5.1	371.9	37.1%
		586	0.8	1.2	4.4	423.8	33.6%
	950	414	4.6	9.3	37.6	164.0	28.0%
		414	0.8	2.5	15.7	159.9	33.7%
		310	9.7	42.6	293.6	706.4	33.8%
		241	26.7	106.1	536.0	1398.1	47.2%
	1100	103	17.0	55.3	351.1	728.5	30.6%

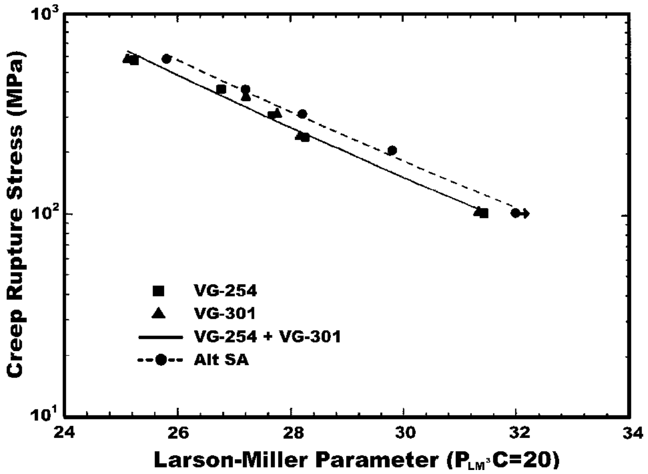

Fig. 4 Larson-Miller parameter plot of creep resistance. Note the increased creep resistance observed in the samples given the alternate solution heat treatment (dashed line) compared to the standard solution anneal (solid line).

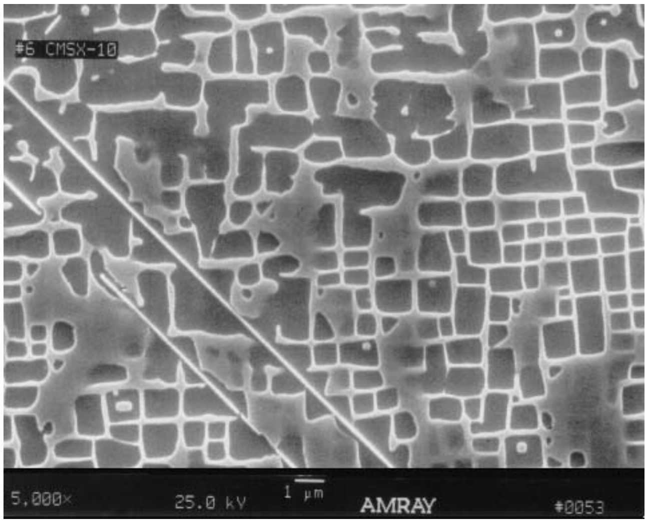

Fig. 5 The TCP phases formed in an unstressed sample aged at 1050 °C for 1000 h

of three samples tested under similar conditions. In addition, creep properties for a second heat of CMSX-10 given both solution anneals also are plotted in Fig. 4 to illustrate the very limited amount of scatter observed in the creep testing. The results, even considering the data scatter, consistently indicated that the alternate solution heat treatment resulted in increased creep resistance. The type of solution heat treatment did not appear to affect the amount of data scatter under the test conditions used, and only a very limited amount of scatter was observed in the creep ductilities observed, regardless of the solution heat treatments and the test conditions.

Microstructural characterization of the creep samples indicated that topologically close-packed (TCP) phases, such as sigma (σ) and *P*, were observed after creep testing at 1100 °C in both the standard and alternate solution heat-treated samples (Fig. 5). However, the TCP phases were present in the grip sections, which were under very low load in both samples, whereas the highly loaded gauge section did not exhibit any TCP phases in any of the samples evaluated in this study. No evidence of TCP phases was observed in the other samples. Similar results were observed in the unstressed long-term heat-treated samples. The TCP phases were observed in the samples that were heat treated at 1050 °C for 1000 and 10,000 h. The solution heat treatment did not appear to affect the formation of the TCP phases, because TCP phases were observed in samples given both the standard and the alternate solution heat treatments.

The SEM fractographic analysis indicated that all samples failed in a ductile shear mode. No evidence of fracture due to defects, such as porosity or TCP phases, was observed in any of the samples. The solution heat treatment did not appear to affect the type of fracture because the fracture surfaces were similar, regardless of the solution heat treatment. The TEM analysis also indicated that the solution heat treatment did not have any effect on the deformation mechanisms or fine microstructures.

4. Discussion

The development of directional solidification to produce single crystals allowed for the removal of the grain-boundary strengthening elements, which also increased the solidus of the alloy.[1,2] Continued development of the single-crystal alloys resulted in alloys with increasing refractory-metal contents and, in particular, increased levels of W and Re. The increased refractory-metal contents resulted in more highly segregated microstructures in the as-cast condition, due to the partitioning of these elements to the dendrite cores. Therefore, the solution heat treatment not only solutions the γ', but also reduces the chemical segregation present in the as-cast microstructure.[8]

Examining the microstructure of the samples following both solution heat treatments indicated that the γ' and the eutectic γ/γ' are completely solutioned in the heat-treatment cycle. However, the chemical segregation from the partitioning of elements to the dendrite core or to the interdendritic areas persists to higher heat-treatment temperatures.[8] In particular, the refractory-metal elements, W and Re, do not exhibit appreciable homogenization until the heat-treatment temperatures reach 1360 °C or above.

The local enrichment of Re and W that occurs in the dendrite core, due to the solidification partitioning, must be reduced or eliminated by the solution heat treatment. These elements participate in the formation of TCP phases, such as σ and *P*, in alloys that are not microstructurally stable and would be expected to result in degraded properties.[12-14] However, local enrichment of elements, such as the enrichment of W, Re, and Cr at the dendrite cores during solidification, can result in precipitation of the deleterious TCP phases in alloys that are compositionally balanced to prevent TCP-phase formation.[15] Therefore, solution heat treatments that do not result in significant reductions in the segregation of these elements are not sufficient to necessarily prevent the formation of the TCP phases in the dendrite cores.[15] In general, higher solution heat-treatment temperatures were observed to result in more complete homogenization, particularly for the elements with slow diffusion rates (i.e., W and Re). Microstructural characterization also indicated that the size of the γ' was unaffected by the solution heat treatment. Both solution heat treatments completely dissolved the γ' at temperatures significantly below the maximum heat-treatment temperature.[8]

The mechanical properties also appeared to be affected by the solution heat treatment. The samples given the alternate solution anneal exhibited strengths at least equivalent to the samples with standard heat treatments. However, the creep strength and ductilities of the samples that received the alternate solution heat treatment were consistently greater that those of the standard heat-treated samples. Because there are no significant changes in the microstructure of the samples after the modified solution heat treatment, the increased creep strength and ductility may be due to the enhanced homogenization of the higher temperatures and longer times spent at higher temperatures.

The increase in strength due to increased homogeneity of the microstructure is not entirely surprising. Previously, the increased creep strength observed in higher temperature solution heat treatments in PWA 1480 was attributed to increased levels of γ/γ' eutectic solutioning.[9] However, in the case of CMSX-10, the γ/γ' eutectic solution occurs at lower temperature, but the W and Re partitioning remains at much higher temperatures. The increased creep resistance and increased ductility appear to be due to the increased chemical homogeneity of the material following the modified solution heat treatment.

5. Conclusions

The standard solution heat treatment of the third-generation, single-crystal Ni-base superalloy, CMSX-10, requires approximately 45 h and temperatures up to 1365 °C. Attempts to shorten the heat-treatment cycle and/or decrease the temperatures may result in a microstructure that is less stable. Therefore, a modified solution heat treatment was examined that was of similar length, but utilized higher heat-treatment temperatures and increased the time spent at higher temperatures. The modified heat treatment resulted in increased levels of chemical homogeneity and also increased creep strength. The higher levels of creep strength and ductility appeared to decrease with increasing test temperature. However, the increased creep strengths and increased ductilities were attributed to increased chemical homogeneity.

Acknowledgment

This material is based upon work supported by the National Science Foundation under Grant No. l0072671.

References

1. “Metallurgy, Processing and Properties of Superalloys,” in *Heat Resistant Materials—ASM Specialty Handbook,* J.R. Davis, ed., ASM International, Materials Park, OH, 1997, pp. 221-254.
2. “Directionally Solidified and Single Crystal Superalloys,” in *Heat Resistant Materials—ASM Specialty Handbook,* J.R. Davis, ed., ASM International, Materials Park, OH, 1997, pp. 255-271.
3. D.N. Duhl: in *Superalloys II,* C.T. Sims, N.S. Stoloff, and W.C. Hagel, ed., Wiley and Sons, New York, 1987.
4. M. Durand-Charee: *The Microstructure of Superalloys,* Gordon and Breach Science Publishers, Canada, 1997, p. 60.
5. F.J. Fela: Master’s Thesis, University of Florida, Gainesville, FL, 2000.
6. G.L. Erickson: *Materials Science and Engineering,* TMS-AIME, Warrendale, PA, 1995, p. 36.
7. T. Khan and P. Caron: “Advanced Single Crystal Ni-base Superalloys,” in *Advances in High Temperature Structural Materials and Protective Coatings,* A.K. Koul, V.R. Parameswaran, J.P. Immarigeon, and W. Wallace, ed., NRC of Canada, Ottawa, Canada, 1994.
8. G.E. Fuchs: “Solution Heat Treatment Response of a Third Generation Single Crystal Ni-base Superalloy,” *Mater. Sci. Eng.,* 2001, *A300,* pp. 52-60.
9. P. Caron and T. Khan: “Improvement in Creep Strength in a Nickel-base Single Crystal Superalloy by Heat-Treatment,” *Mater. Sci. Eng.,* 1983, *61*, p. 173.
10. D.L. Sponseller: “Differential Thermal Analysis of Nickel-Base Superalloys,” in *Superalloys 1996,* R.D. Kissinger, D.J. Deye, D.L. Anton, A.D. Cetel, M.V. Nathal, T.M. Pollock, and D.A. Woodford, ed., TMS, Warrendale, PA, 1996.
11. T.M. Pollock, W.H. Murphy, E.H. Goldman, D.L. Uram, and J.S. Tu: “Grain Defect Formation during Directional Solidification of Nickel Base Single Crystal Superalloys,” in *Superalloys 1988,* S.D. Antolovich, R.W. Sustrud, R.A. MacKay, D.L. Anton, T. Khan, R.D. Kissinger, and D.L. Klarstrom, ed., TMS, Warrendale, PA, 1992.
12. W.S. Walston, J.C. Shaeffer, and W.H. Murphy: “A New Type of Microstructural Instability in Superalloys–SRZ,” in *Superalloys 1996,* R.D. Kissinger, D.J. Deye, D.L. Anton, A.D. Cetel, M.V. Nathal, T.M. Pollock, and D.A. Woodford, ed., TMS, Warrendale, PA, 1996.
13. E.W. Ross and K.S. O’Hara: “René N4: A First Generation Single Crystal Turbine Airfoil Alloy with Improved Oxidation Resistance, Low Angle Boundary Strength and Superior Long Time Rupture Strength,” in *Superalloys 1996,* R.D. Kissinger, D.J. Deye, D.L. Anton, A.D. Cetel, M.V. Nathal, T.M. Pollock, and D.A. Woodford, ed., TMS, Warrendale, PA, 1996.
14. S.T. Wlodek: “The Stability of Superalloys,” in *Long Term Stability of High Temperature Materials,* G.E. Fuchs, K.A. Dannemann, and T.C. Deragon, ed., TMS, Warrendale, PA, 1999.
15. W.S. Walston, K.S. O’Hara, E.W. Ross, T.M. Pollock, and W.H. Murphy: “René N6: Third Generation Single Crystal Superalloy,” in *Superalloys 1996,* R.D. Kissinger, D.J. Deye, D.L. Anton, A.D. Cetel, M.V. Nathal, T.M. Pollock, and D.A. Woodford, ed., TMS, Warrendale, PA, 1996.